JOURNAL OF AGRICULTURAL AND FOOD CHEMISTRY

Pterostilbene Induces Apoptosis and Cell Cycle Arrest in Human Gastric Carcinoma Cells

MIN-HSIUNG PAN,*,† YEN-HUI CHANG,† VLADIMIR BADMAEV,‡ KALYANAM NAGABHUSHANAM,‡ AND CHI-TANG HO§

Department of Seafood Science, National Kaohsiung Marine University, Kaohsiung 811, Taiwan; Sabinsa Corporation, 70 Ethel Road West Unit 6, Piscataway, New Jersey 08854; and Department of Food Science, Rutgers University, New Brunswick, New Jersey 08901

Pterostilbene, an active constituent of blueberries, is known to possess anti-inflammatory activity and also induces apoptosis in various types of cancer cells. Here, the effects of pterostilbene on cell viability in human gastric carcinoma AGS cells were investigated. This study demonstrated that pterostilbene was able to inhibit cell proliferation and induce apoptosis in a concentration- and time-dependent manner. Pterostilbene-induced cell death was characterized with changes in nuclear morphology, DNA fragmentation, and cell morphology. The molecular mechanism of pterostilbene-induced apoptosis was also investigated. The results show the caspase-2, -3, -8, and -9 are all activated by pterostilbene, together with cleavage of the downstream caspase-3 target DNA fragmentation factor (DFF-45) and poly(ADP-riobse) polymerase. Moreover, the results indicate that the Bcl-family of proteins, the mitochondrial pathway, and activation of the caspase cascade are responsible for pterostilbene-induced apoptosis. Pterostilbene markedly enhanced the expression of growth arrest DNA damage-inducible gene 45 and 153 (GADD45 and GADD153) in a time-dependent manner. Flow cytometric analysis indicated that pterostilbene blocked cell cycle progression at G1 phase in a dose- and time-dependent manner. Pterostilbene increased the p53, p21, p27, and p16 proteins and decreased levels of cyclin A, cyclin E, cyclin-dependent kinase 2 (Cdk2), Cdk4, and Cdk6, but the expression of cyclin D1 was not affected. Over a 24 h exposure to pterostilbene, the degree of phosphorylation of Rb was decreased after 6 h. In summary, pterostilbene induced apoptosis in AGS cells through activating the caspase cascade via the mitochondrial and Fas/FasL pathway, GADD expression, and by modifying cell cycle progress and changes in several cycle-regulating proteins. The induction of apoptosis by pterostilbene may provide a pivotal mechanism of the antitumor effects and for treatment of human gastric cancer.

KEYWORDS: Pterostilbene; apoptosis; cell cycle

INTRODUCTION

Pterostilbene (*trans*-3,5-dimethoxy-4′-hydroxystilbene), a dimethyl ether analogue of resveratrol, was found to be as effective as resveratrol in preventing carcinogen-induced preneoplastic lesions in a mouse mammary culture model and inhibited metastatic growth of melanoma cells to the liver (*1, 2*). Pterostilbene has been demonstrated to have a cancer chemopreventive activity similar to that of resveratrol, and it is cytotoxic to a number of cancer cell lines (*2, 3*). Pterostilbene, isolated from *Vaccinium* barriers, together with resveratrol, suppressed aberrant crypt foci formation in the azoxymethane-induced colon carcinogenesis in rats (*4, 5*).

Gastric adenocarcinoma is a global health problem and is ranked the second cause of cancer-related death in the world (*6*). Studies have shown that a high intake of smoked, salted, and nitrated foods and a high intake of carbohydrates, but a low intake of vegetables, fruits, and milk, are linked to cancer incidence. These diets have been shown to significantly increase the risk for stomach cancer (*7*). Epidemiological studies have provided convincing evidence that dietary factors can modify the processes of carcinogenesis, including initiation, promotion, and progression of several types of human cancer (*8*). The occurrence of gastrointestinal (GI) cancers has increased during the past decade. For instance, colorectal cancer is the second leading cause of cancer mortality in Western societies (*9*) and one of the world's most common malignancies (*10, 11*). The fight against GI cancer is an important global issue.

* To whom correspondence should be addressed (Tel.: (886)-7-361-7141. Ext. 3623; Fax: (886)-7-361-1261; E-mail mhpan@mail.nkmu.edu.tw).
† National Kaohsiung Marine University.
‡ Sabinsa Corporation.
§ Rutgers University.

10.1021/jf071520h CCC: $37.00
Published on Web 08/16/2007

Apoptosis is a defined type of cell death and differs from traditional cell death, necrosis. There are two main pathways involving apoptotic cell death. First, it is the interaction of the cell surface receptors, such as Fas, tumor necrosis factor receptor (TNFR), death receptor 3 (DR3), TNF-related apoptosis-inducing ligand–receptor 1 (TRAIL-R1 or DR4), and R2 (DR5), with their ligands. Second, it is involved in the participation of mitochondria, for most forms of apoptosis in response to cellular stress, loss of survival factors, and developmental cues (*12, 13*). Recent studies of the endoplasmic reticulum (ER) as a third subcellular compartment containing caspase-12 were implicated in apoptotic execution induced by ER stress (*14–16*).

The molecular mechanisms of cell cycle arrest by naturally occurring phenolic compounds, such as stilbenes, remain largely unclear but appear to involve modulation of multiple cell cycle regulatory proteins. The eukaryotic cell cycle is regulated through the sequential activation and inactivation of cyclin-dependent kinases (Cdks) that drive cell cycle progression through the phosphorylation and dephosphorylation of several regulatory proteins (*17*).

A previous study showed that pterostilbene inhibited proliferation and induced apoptosis in human leukemia cells (*3*). However, to date, no information is available regarding the mechanism of the effects of pterostilbene on human gastric cancer. In this study, the mechanism of apoptosis was investigated. This included studies on the effects of pterostilbene on the activation of caspase cascade, expression of Bax, Bxl-X_L, and Bad, the distribution of cells in the cell cycle, and changes in expression of cycle-regulating proteins (cyclin A, D, and E and the cyclin-dependent kinase 2, 4, and 6), p53, p21, p27, p16, and GADD in gastric carcinoma cells.

MATERIALS AND METHODS

Cell Culture and Chemicals. Human promyelocytic leukemia (HL-60) cells obtained from American type Culture Collection (Rockville, MD), COLO 205 cells, and HT-29 cells were grown in RPMI 1640 medium and 10% fetal bovine serum (Gibco BRL, Grand Island, NY) supplemented with 2 mM glutamine (Gibco BRL) and 1% penicillin/streptomycin (10000 units of penicillin/mL and 10 mg/mL streptomycin). HepG2 cell line was derived from human hepatocellular carcinoma (ATCC HB-8065). Human polymorphonuclear cells (PMNs) were obtained from healthy male donors and were separated by the Ficoll-Hypaque density gradient. Human PMNs were washed twice in 0.9% NaCl and resuspended in RPMI-1640 medium. The human AGS gastric carcinoma cells (CCRC 60102) were obtained from the Food Industry Research and Development Institute (Hsinchu, Taiwan) and cultured in Dulbecco's modified Eagle's medium/Nutrient mixture F-12 containing 10% heat inactivated fetal bovine serum (Gibco BRL, Grand Island, NY), 100 units/mL of penicillin, 100 μg/mL of streptomycin, and 2 mM L-glutamine (Gibco BRL) and kept at 37 °C in a humidified 5% CO_2 incubator. Pan-caspase inhibitor (z-Val- Ala-Asp-fluoromethyl ketone, z-VAD-FMK) was purchased from Calbiochem (La Jolla, CA). Propidium iodide was obtained from Sigma Chemical Co. (St. Louis, MO). Propidium iodide was obtained from Sigma Chemical Co. (St. Louis, MO). Pterostilbene was synthesized according to the method reported by Pettit et al. (*18*). The purity of pterostilbene was determined by HPLC as higher than 99.2%.

Cell Proliferation Assay. Cell viability was assayed by 3-(4,5-dimethylthiazol-2-yl)-2,5-diphenyltetrazolium bromide (MTT). Briefly, human cancer cells were plated at a density of 1×10^5 cells/mL into 24 well plates. After overnight growth, cells were pretreated with a series of concentration of pterostilbene for 24 h. The final concentration of dimethyl sulfoxide (DMSO) in the culture medium was <0.05%. At the end of treatment, 30 μL of MTT was added, and the cells were incubated for a further 4 h. Cell viability was determined by scanning with an enzyme-linked immunosorbent assay reader with a 570 nm filter (*19*).

DNA Extraction and Electrophoretic Analysis. The AGS cells were harvested, washed with phosphate-buffered saline (PBS), and then lysed overnight at 56 °C with a digestion buffer containing 0.5% sarkosyl, 0.5 mg/mL proteinase K, 50 mM tris(hydroxymethyl)aminomethane (pH 8.0), and 10 mM ethylenediaminetetraacetic acid (EDTA). Following this lyses, the cells were then treated with RNase A (0.5 μg/mL) for 3 h at 56 °C. The DNA was then extracted using phenol/chloroform/isoamyl alcohol (25:24:1) prior to loading and was analyzed by 2% agarose gel electrophoresis. The agarose gels were run at 50 V (20 mA) for 120 min in Tris-borate/EDTA electrophoresis buffer. Approximately 20 μg of DNA was loaded into each well, DNA was stained with ethidium bromide and visualized under UV light (260 nm), and the plates were photographed (*20*).

Acridine Orange Staining Assay. Cells (5×10^5) were seeded into 60 mm Petri dishes and incubated at 37 °C for 24 h. The cells were harvested, and 5 μL of suspended cells was mixed on a slide with an equal volume of acridine orange solution (10 μg/mL in PBS). Green fluorescence was detected between 500 and 525 nm by using an Olympus fluorescence microscope (CK40) (Olympus America, Inc., Lake Success, NY). Bright-staining condensed chromatin was detected in apoptotic cells.

Flow Cytometry. HL-60 cells (2×10^5) were cultured in 60 mm Petri dishes and incubated for 24 h. The cells were then harvested, washed with PBS, resuspended in 200 μL of PBS, and fixed in 800 μL of iced 100% ethanol at −20 °C. After being left to stand overnight, the cell pellets were collected by centrifugation, resuspended in 1 mL of hypotonic buffer (0.5% Triton X-100 in PBS and 0.5 μg/mL RNase), and incubated at 37 °C for 30 min. Next, 1 mL of propidium iodide solution (50 μg/mL) was added, and the mixture was allowed to stand on crushed water ice for 30 min. Fluorescence emitted from the propidium iodide–DNA complex was quantitated after excitation of the fluorescent dye by FACScan cytometry (Becton Dickinson, San Jose, CA). Quantitation of the fraction of each cell cycle stage was performed with ModFit LT for Mac 3.0 software (Becton Dickinson, San Jose, CA).

ROS Production Determination. Cells were treated with pterostilbene (80 μM) for different time periods, and DCFH-DA (20 μM) or DHE (20 μM) was added to the medium for a further 30 min at 37 °C. ROS production was monitored by flow cytometry using DCFH-DA. This dye is a stable, nonpolar compound that readily diffuses into cells and is hydrolyzed by intracellular esterase to yield DCFH, which is trapped within the cells. Hydrogen peroxide or low molecular weight peroxides produced by the cells oxidize DCFH to the highly fluorescent compound 2′,7′-dichlorofluorescein (DCF). Thus, the fluorescence intensity is proportional to the amount of peroxide produced by the cells.

Analysis of Mitochondrial Transmembrane Potential. The change of the mitochondrial transmembrane potential was monitored by flow cytometry. Briefly, AGS cells were exposed to pterostilbene (80 μM) for different time periods, and the mitochondrial transmembrane potential was measured directly using 40 nM 3,3′-dihexyloxacarbocyanine [DiOC6(3)] (Molecular Probes, Eugene, OR). Fluorescence was measured after staining the cells for 30 min at 37 °C. Histograms were analyzed using Cell Quest software and were compared with histograms of untreated, control cells.

Western Blotting. For the determination of the expression of Bcl-2 family, cytochrome *c*, GADD 45, and GADD153 protein, the nuclear and cytosolic proteins were isolated from AGS cells after treatment with 80 μM pterostilbene for the indicated time points. The total proteins were extracted via the addition of 200 μL of gold lysis buffer (50 mM Tris-HCl, pH 7.4, 1 mM NaF, 150 mM NaCl, 1 mM EGTA, 1 mM phenylmethanesulfonyl fluoride; 1% NP-40; and 10 μg/mL leupeptin) to the cell pellets on ice for 30 min, followed by centrifugation at 10000*g* for 30 min at 4 °C. The cytosolic fraction (supernatant) proteins were measured by the Bio-Rad protein assay (Bio-Rad Laboratories, Munich, Germany). The samples (50 μg of protein) were mixed with 5 × sample buffer containing 0.3 M Tris-HCl (pH 6.8), 25% 2-mercaptoethanol, 12% sodium dodecyl sulfate (SDS), 25 mM EDTA, 20% glycerol, and 0.1% bromophenol blue. The mixtures were boiled at 100 °C for 5 min and were prerun on a stacking gel and then resolved by 12% SDS–polyacrylamide

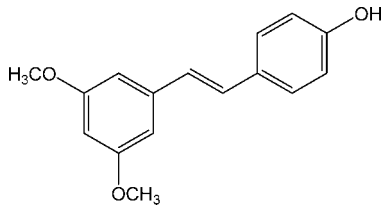

Figure 1. Chemical structure of *trans*-3,5-dimethoxy-4′-hydroxystilbene (pterostilbene).

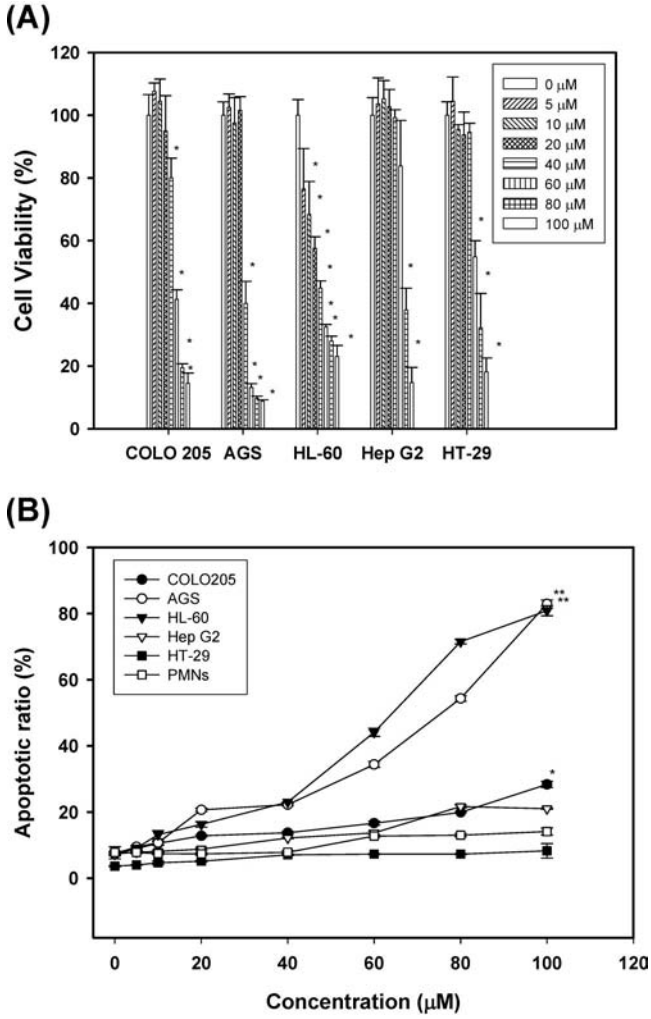

Figure 2. Effect of pterostilbene on the growth and apoptosis of various human cancer cells. Cells were treated with various concentrations of pterostilbene for 24 h. (A) Cell viability was then determined by MTT assay. (B) The apoptotic ratio (%) was determined by flow cytometry. Cells were treated with 0.05% DMSO as vehicle control. Data are mean ± SD of two independent experiments in triplicate. *Significantly different compared with control (*$P < 0.05$ and **$P < 0.01$).

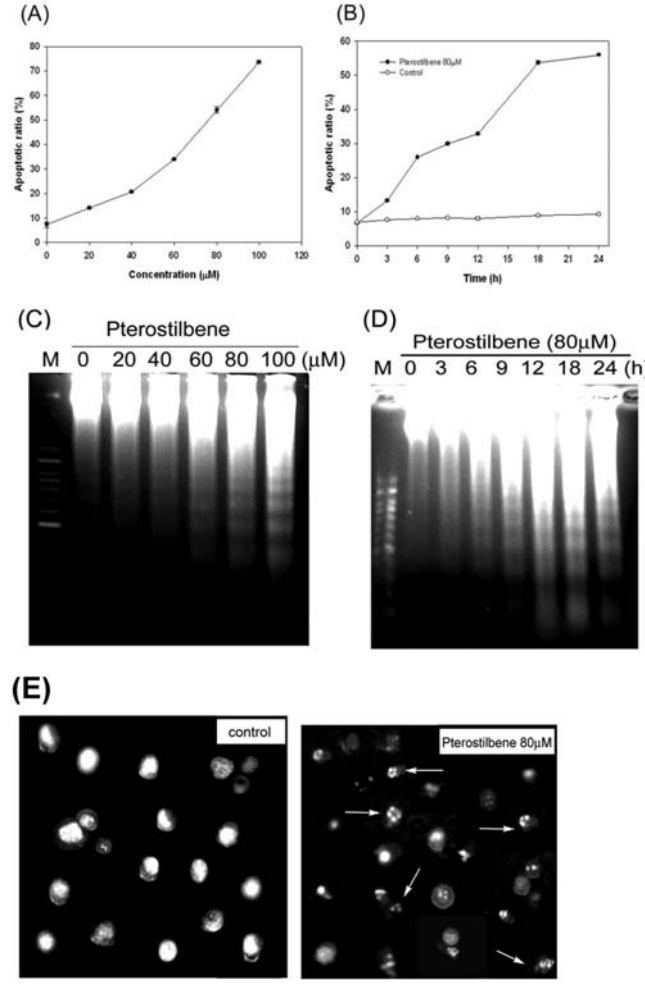

Figure 3. Induction of DNA fragmentation and chromatin condensation by pterostilbene in AGS cells. (A) AGS cells treated with increasing doses of pterostilbene for 24 h or (B) treated with 80 μM pterostilbene for the indicated time and then determination of sub-G1 cells by flow cytometry. (C) AGS cells were treated with different concentrations of pterostilbene for 24 h or (D) treated with 80 μM pterostilbene for indicated time. DNA fragmentation was analyzed by 2% agarose electrophoresis (M: 100 base pair DNA ladder size marker.) Cells were treated 0.05% DMSO as vehicle control. The data were represented as means ± SD for three determinations. (E) The chromatin condensation were induced by pterostilbene in AGS cells. AGS cells were treated with 0.05% DMSO as vehicle control or treated with 80 μM pterostilbene for 24 h, and cells were harvested and washed with PBS following by staining with acridine orange. The nuclear staining was examined by fluorescence microscope (200×). The cell nuclear condensation is shown as arrowheads. These experiments were performed at least in triplicate, and a representative experiment is presented.

minigels at a constant current of 20 mA. Subsequently, electrophoreses were carried out on SDS–polyacrylamide gels. For electrophoresis, proteins on the gel were electrotransferred onto a 45 μm immobile membrane (PVDF; Millipore Corp., Bedford, MA) with transfer buffer composed of 25 mM Tris-HCl (pH 8.9), 192 mM glycine, and 20% methanol. The membranes were then blocked with blocking solution (20 mM Tris-HCl pH 7.4, 0.2% Tween 20, 1% bovine serum albumin, and 0.1% sodium azide). The membrane was further incubated with the respective specific antibodies at the appropriate dilution (1:1000) using various blocking solution, such as anti-Bad, anti-Bcl-X_L, anti-Bax, anti-GADD45, anti-GADD153, anti-β-actin (Santa Cruz Biotechnology), anti-PARP (UBI, Inc., Lake Placid, NY), anti-Bid (Transduction Laboratory, Lexington, KY), anti-DFF 45/inhibitor of caspase-activated DNase (ICAD) antibody (MBL, Naka-Ku, Nagoya, Japan), and antibodies including Rb, p53, p21, p27, p16, cyclin A1, cyclin D1, cyclin E, Cdk2, Cdk4, Cdk6, and β-actin (Transduction Laboratory, Lexington, KY) at room temperature for 1 h. The membranes were subsequently probed with anti-mouse or anti-rabbit IgG antibody conjugated with horseradish peroxidase (Transduction Laboratories, Lexington, KY), and detection was achieved by measuring the chemiluminescence of the blotting agents (ECL, Amersham Corp., Arlington Heights, IL) by exposure of the filters to Kodak X-Omat films. The densities of the bands were quantitated with a computerized densitometer system (AlphaImager 2200 system, Alpha Innotech Corp., San Leandro, CA). The mitochondrial and cytosolic fractions isolated from the

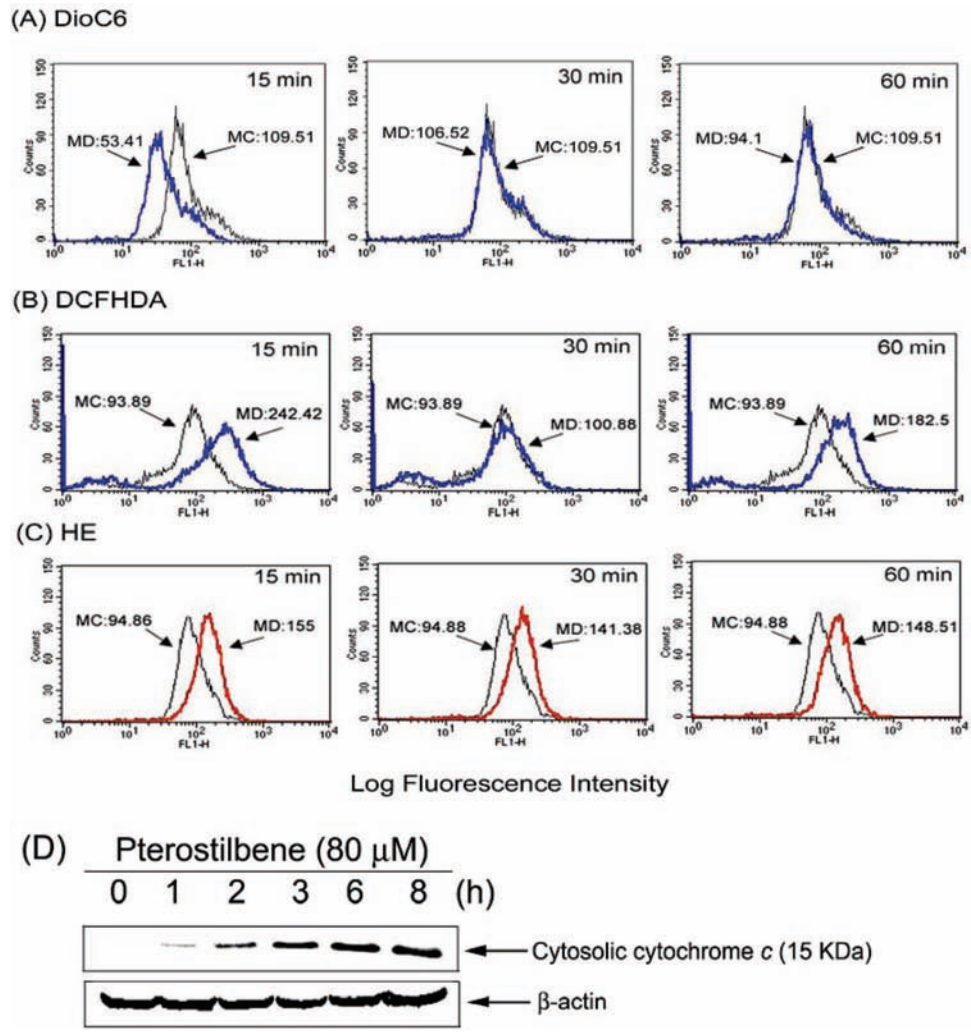

Figure 4. Induction of mitochondrial dysfunction, reactive oxygen species (ROS) generation, and cytochrome *c* release in pterostilbene-induced apoptosis. (A) AGS cells were treated with 80 μM pterostilbene for indicated times and were then incubated with (A) 3,3′-dihexyloxacarbocyanine (40 nM), (B) DCFH–DA (20 μM), and (C) DHE (20 μM) and analyzed by flow cytometry. Data are presented as log fluorescence intensity (MC: means control cells; MD: represents cell drugged). (D) AGS cells were treated with 80 μM pterostilbene at indicated periods. Cytosolic cytochrome *c* was detected by cytochrome *c* antibody as described in the Materials and Methods section. These experiments were performed at least in triplicate, and a representative experiment is presented.

cells were used for immunoblot analysis of cytochrome *c* as previously described (*21*). The cytochrome *c* protein was detected using an anti-cytochrome *c* antibody (Research Diagnostic Inc., Flanders, NJ).

Activity of Caspase. Cells were collected and washed with PBS and suspended in 25 mM HEPES (pH 7.5), 5 mM $MgCl_2$, 5 mM EDTA, 5 mM dithiothione, 2 mM phenylmethanesulfonyl fluoride, 10 μg/mL pepstatin A, and 10 μg/mL leupeptin after treatment. Cell lysates were clarified by centrifugation at 12000*g* for 20 min at 4 °C. Caspase activity in the supernatant was determined by a fluorogenic assay (Promeaga's CaspACE Assay System Corp., Madison, WI). Briefly, 50 μg of total protein, as determined by the Bio-Rad protein assay kit (Bio-Rad Laboratories, Hercules, CA 94547), was incubated with 50 μM substrate Ac-Try-Val-Ala-Asp-AMC (Ac-YVAD-AMC, caspase-1 specific substrate), Ac-Val-Asp-Val-Ala-Asp-AMC (Ac-VDVAD-AMC, caspase-2-specific substrate), Ac-Asp-Glu-Val-Asp-AMC (Ac-DEVD-AMC, caspase-3 specific substrate), Ac-Ile-Glu-Thr-Asp-AMC (Ac-IETD-AMC, caspase-8 specific substrate), or Ac-Leu-Glu-His-Asp-AMC (Ac-LEHD-AMC, caspase-9 specific substrate) at 30 °C for 1 h. The release of methylcoumaryl-7-amine (AMC) was measured by excitation at 360 nm and emission at 460 nm using a fluorescence spectrophotometer (ECLIPSE, Varian, Palo Alto, CA).

Statistical Analysis. Data are presented as means ± standard deviation (SD). Statistical significance was examined using the Student's *t*-test comparison between the means. A P value of <0.05 was considered statistically significant.

RESULTS

Inhibition of Cell Proliferation in Pterostilbene-Treated Human Cancer Cells. We first compared the effects of pterostilbene (**Figure 1**) on the growth of human cancer cells using the MTT assay, as previously described. As shown in **Figure 2A**, pterostilbene decreased cell growth in cultured human cancer cells (COLO 205, AGS, HL-60, HepG2, and HT-29) in a dose-dependent manner, but not cytotoxicity in primary human PMNs cells analyzed using trypan blue exclusion (data not shown), with IC_{50} values of 71.2, 50.7, 46.7, 82.8, and 71.8 μM, respectively. The cell-growth inhibitory effect on AGS cells was sensitive to pterostilbene (60 μM) as compared to COLO 205, HL-60, HepG2, and HT-29 cells. To investigate the induction of apoptotic cells, the DNA content of various human cancer cells treated with pterostilbene using flow cytometry. As shown in **Figure 2B**, pterostilbene has its strongest apoptosis-inducing effect on AGS (100 μM). As a result, we further examined the cytotoxic effects of pterostilbene in AGS cells.

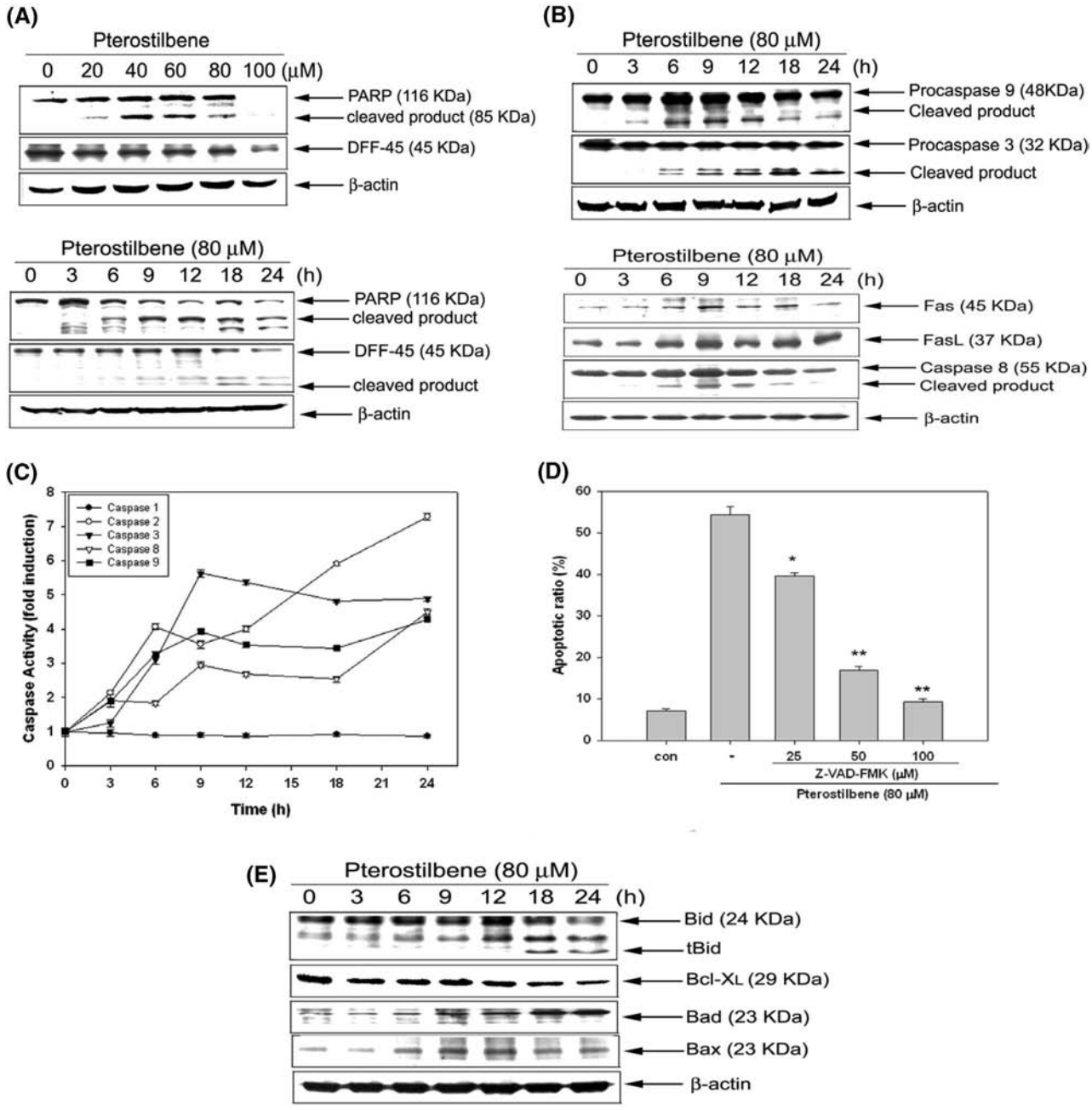

Figure 5. Induction of caspase activity through decrease and cleavage of procaspase-9 and -3 during pterostilbene-induced apoptosis in AGS cells. (A) Dose- and time-dependent cleavage of PARP and DFF-45 induced by pterostilbene. (B) AGS cells were treated 80 μM pterostilbene for indicated time, and the expressions of caspase-3, -9, -8, Fas, and FasL were analyzed by Western blotting as described in the Materials and Methods section. (C) Kinetics of caspase activation; cells were treated 80 μM pterostilbene for indicated time periods. The cells were harvested and lysed in lysis buffer. Enzymatic activities of caspase-1, -2, -3, -8, and -9 were determined by incubation of 50 μg of total protein with specific fluorogenic substrates for 1 h in 30 °C. The release AMC was monitored with excitation = 360 nm and emission = 460 nm. Data represent means ± SD for three determinations. (D) AGS cells were pretreated with pan-caspase inhibitor Z-VAD-FMK (25, 50, and 100 μM, respectively) for 1 h followed by pterostilbene for another 24 h. The apoptotic ratio (%) was detected by flow cytometry. Each experiment was independently performed in triplicate and expressed as mean ± SD. Asterisk denotes a statistically significant decrease compared with values of positive control (*P < 0.05, **P < 0.01). (E) Effect of pterostilbene on Bcl-2 family protein expression in AGS cells. AGS cells were treated with 80 μM pterostilbene for indicated time point. Western blot analyses of Bid, Bcl-X_L, Bad, and Bax expressions in AGS cells as described in the Materials and Methods section. These experiments were performed at least in triplicate, and a representative experiment is presented.

Pterostilbene Induces Apoptosis in Human Gastric Carcinoma Cells. Physiological cell death is characterized by apoptotic morphology, including chromatin condensation, membrane blebbing, inter-nucleosomal degradation of DNA, and apoptotic body formation. To investigate whether the cytotoxic effects of pterostilbene observed in AGS cells were due to apoptotic cell death, cells were treated with pterostilbene (5–100 μM) for 24 h or 80 μM for different times, and the sub-G1 cell population, a hallmark of apoptosis, was performed by flow cytometry. As seen in **Figure 3A**,**B**, pterostilbene was able to induce apoptosis in a concentration- and time-dependent manner. We further evaluated the potential mechanism of the cytotoxic effects; AGS cells were treated with various concentrations of pterostilbene for 24 h or 80 μM pterostilbene for several periods

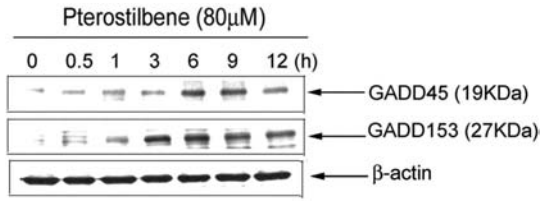

Figure 6. Effect of pterostilbene treatment on protein levels of GADD45 and GADD153. AGS cells were incubated with 80 μM pterostilbene for the different time periods indicated. Then, whole cell lysates were prepared for subsequent Western blotting. The GADD45 and GADD153 proteins were detected using specific antibodies. These experiments were performed at least in triplicate, and a representative experiment is presented.

followed by DNA fragmentation analyses. As shown in **Figure 3C**,**D**, significant DNA ladders were observed in AGS cells after 60 μM of pterostilbene treatment for 24 h. After treatment with 80 μM pterostilbene for 6 h, digested genomic DNA was evident. The cell death induced by pterostilbene was characterized by examining the nuclear morphology of dying cells using a fluorescent DNA-binding agent, acridine orange. With 24 h of treatment with 80 μM pterostilbene, cells clearly exhibited significant morphological changes and chromosomal condensation, indicative of apoptotic cell death (**Figure 3E**). The observed effect of pterostilbene on increases in the percentage of apoptotic cells, DNA laddering, morphological changes, and chromosomal condensation links the cytotoxic action of pterostilbene to an ability to induce apoptosis.

Involvement of Mitochondrial Dysfunction, ROS Production, and Release of Cytochrome *c* from Mitochondria to Cytosol in Pterostilbene-Induced Apoptosis. It has been recently demonstrated that apoptosis involves the disruption of mitochondrial membrane integrity, a mechanism that is decisive for the cell-death process (*22*). The effects of pterostilbene on the mitochondrial transmembrane potential ($\Delta\Psi_m$) and release of mitochondrial cytochrome *c* into cytosol were evaluated. A DiOC6(3) probe monitored via flow cytometry was used to measured $\Delta\Psi_m$ fluorescence. Results of measuring fluorescence intensity in AGS cells exposed to pterostilbene compared to untreated control cells are summarized in **Figure 4A**. The DiOC6(3) fluorescence intensity shifted to the left from 109.51 to 53.41 in pterostilbene-induced apoptotic AGS cells at 15 min. These results confirmed that pterostilbene causes a decrease in the mitochondrial transmembrane potential in AGS cells. The role of ROS in the induction of apoptosis is well recognized (*23*). Results of flow cytometry analysis using DCFH–DA and DHE as fluorescent ROS, H_2O_2, and O_2 indicators demonstrated an increase in intracellular peroxide levels in pterostilbene-treated AGS cells. As shown in **Figure 4B**,**C**, increases of intracellular peroxide levels caused by treatment with pterostilbene were detected at 15 min and markedly increased the mean DCFH–DA fluorescence intensity from 93.89 to 242.42 and DHE fluorescence intensity from 94.86 to 155. The increase in the mean DCFH–DA fluorescence intensity suggests that an increase in ROS concentrations plays an important role as an early mediator in pterostilbene-induced apoptosis. These findings indicate that pterostilbene has an effect on mitochondrial function and the accumulation of ROS. The features are indicative of the induction of apoptosis. Caspase-9 binds to Apaf-1 in a cytochrome *c* and dATP-dependent fashion to become activated and, in turn, cleaves and activates caspase-3 (*24*). As shown in **Figure 4D**, the release of mitochondrial cytochrome *c* into the cytosol was detected at 1 h in pterostilbene-treated AGS cells. The sum of these observations provides clear evidence that pterostilbene-induced apoptosis, most likely triggered by production of ROS, which in turn induces dissipation of mitochondrial membrane potential, releases cytochrome *c* followed by activation of caspase-9.

Effects of Pterostilbene on the Induction of Cleavage, Activation of Caspase Activity, and Fas/Fas-L Apoptotic Pathway. The caspases are believed to play a central role in causing apoptosis by cleaving or degrading several cellular substrates (*25*). Activation of caspase-3 causes the cleavage of poly-(ADP-ribose)-polymerase (PARP), a major indicator enzyme of apoptosis, to produce an 85 kDa fragment during apoptosis. As already described, ICAD is a mouse homologue of human DFF-45. Caspase-3 cleaves DFF-45, and once caspase-activated, deoxyribonuclease (CAD) is released, it can enter the nucleus, where it degrades chromosomal DNA to produce interchromosomal DNA fragments (*26*, *27*). **Figure 5A** shows that the exposure of AGS cells to pterostilbene causes the degradation of 116 kDa PARP into 85 kDa fragments and induces the degradation of DFF-45 protein in a dose- and time-dependent manner. These protein cleavages were associated with the cleavage of pro-caspase-9 and pro-caspase-3 occurring at 6 h and sequentially in AGS cells exposed in a time-dependent manner by pterostilbene (**Figure 5B**). To assess whether pterostilbene promoted apoptosis via receptor-mediated pathway, the Fas and Fas ligand (FasL) protein levels were determined by Western blotting. The result showed that pterostilbene could stimulate the expression of Fas and FasL after treatment with pterostilbene. Maximum Fas and FasL was detected at 9 h (**Figure 5B**). Engagement of Fas and FasL results in the clustering of intracellular death domains of Fas and of Fas-associated death domain (FADD) and pro-caspase-8 into the death-inducing signal complex (DISC), where caspase-8 is activated (*28*). To verify whether the activation of caspase-8 was associated with Fas and FasL production in response to pterostilbene treatment, the cleavage of caspase-8 was detected after treatment of AGS cells with 80 μM pterostilbene at the indicated time points. To monitor the enzymatic activity of caspase-1, -2, -3, -8, and -9, caspase activity was measure following treatment of AGS cell with 80 μM pterostilbene for several periods. As shown in **Figure 5C**, pterostilbene induced a dramatic increase in caspase-2, -3, -8, and -9 activity in a time-dependent manner, but the data showed only a very low level of caspase-1 activity following pterostilbene treatment. To further determine whether the activation of caspase is necessary for pterostilbene-induced apoptosis, a pan-caspase inhibitor, z-VAD-FMK, was used to block intracellular protease, and pterostilbene-induced apoptosis was then analyzed by flow cytometry. Results shown in **Figure 5D** indicated that the pan-caspase inhibitor was dose dependently inhibited pterostilbene-induced apoptosis. Next, we examined the expression of Bcl-2 family proteins at different time points in pterostilbene-treated cell. As shown in **Figure 5E**, the cleavage of Bid protein was detected at 18 h. A slight decrease of Bxl-X_L expression at 18 h was detected; however, there was marked change in the expression of Bad in pterostilbene-treated cells at 18 h. A marked increase of Bax protein at 6 h was detected. These results suggest a potential involvement of Bid, Bad, and Bax protein in pterostilbene-induced apoptosis in AGS cells.

Effect of Pterostilbene on the Expression of GADD in AGS Cells. Western blotting revealed an increase expression of GADD in AGS cells. The expressions of GADD45 and GADD153 were increased in AGS cells following pterostilbene treatment. The increase in expression of GADD45 and GADD153 were in a time-dependent manner (**Figure 6**).

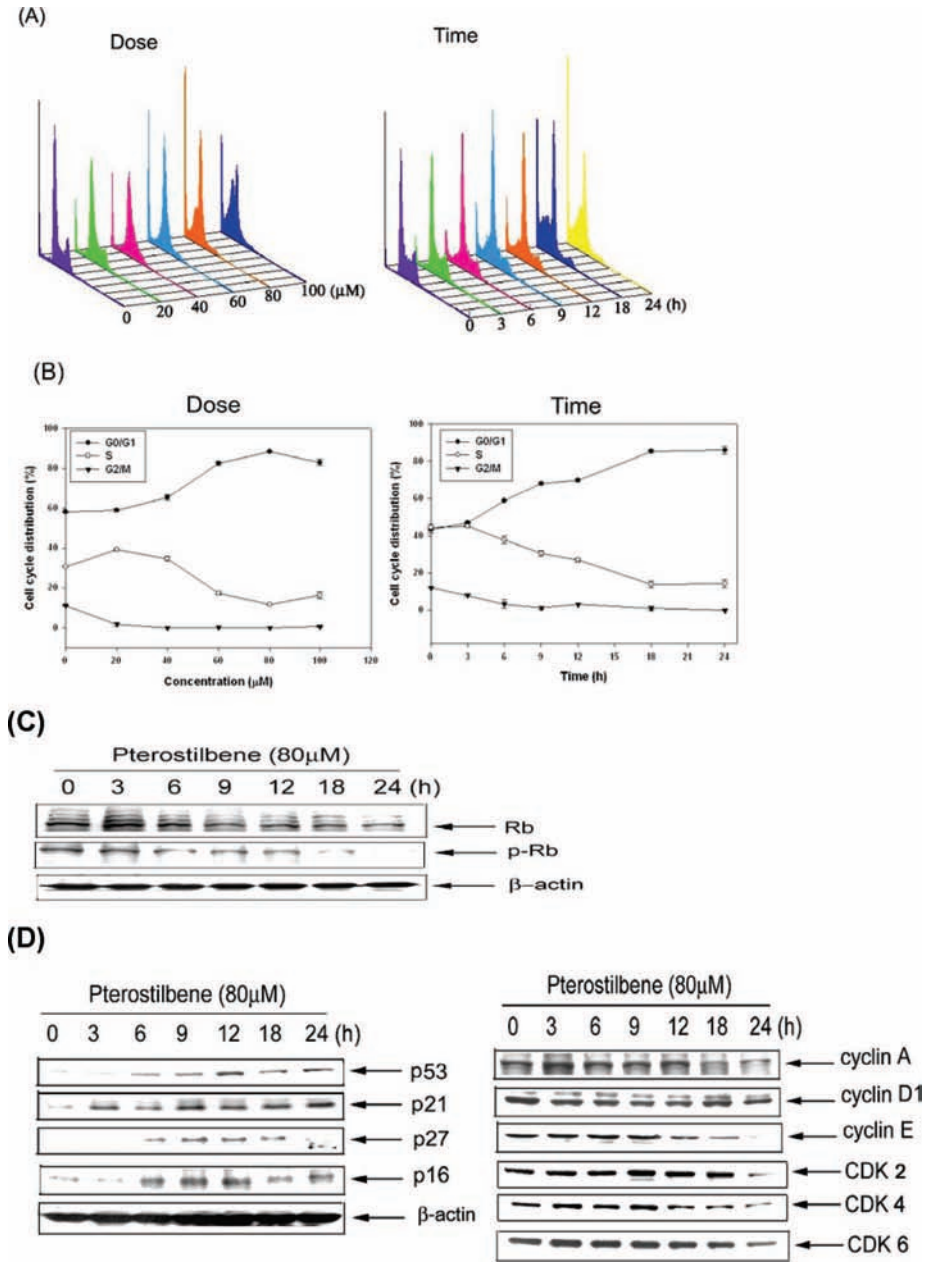

Figure 7. Effect of pterostilbene treatment on cell cycle and the protein expression in AGS cells. (A, B) Cell cycle analysis with performed by flow cytometry as detailed in the Materials and Methods section. The labeled cells were analyzed using FACScan benchtop cytometer, and percentages of cells in the G_0/G1, S, and G2/M phases were calculated using ModFit LT software. The data shown here are from a typical experiment repeated three times, and values represent the means ± SD. (C) AGS cells were treated with 80 μM pterostilbene for the time indicated (top). The phosphorylated Rb and total Rb protein were detected with specific antibodies. (D) AGS cells were treated with 80 μM pterostilbene for different time periods. The cell lysis and Western blotting were performed as indicated in the Materials and Methods section. The data shown here are from a representative experiment repeated in triplicate with similar results.

Molecular Mechanisms of Pterostilbene-Induced G_0/G_1 Arrest. In this study, we demonstrated that pterostilbene induced significant growth inhibition of human gastric carcinoma cells (**Figure 2**). In order to determine whether pterostilbene has a cell cycle arrest effect in AGS cells, the cells treated with different concentrations of pterostilbene for 24 h, or 80 μM pterostilbene for different time periods were subjected to flow cytometric analysis after staining their DNA. As shown in **Figure 7A**,**B**, pterostilbene-treated AGS cells were significantly blocked in the G_0/G_1 phase in a dose- and time-dependent manner. The phosphorylation mediated by both cyclin D/Cdk4 and cyclinE/Cdk2 of the Rb protein is required for the cells to progress from G_1 into S phase in those cells possessing a functional pRb. To elucidate the arrest point of pterostilbene-treated AGS cells in G1 phase, we analyzed the phosphorylation state of pRb, the expression of Cdk inhibitor protein family, and G_1 cyclin protein and Cdks 2, 4, and 6. As shown in **Figure 7C**, the degree of phosphorylation of Rb was decreased after 6 h of 80 μM pterostilbene treatment compared with total Rb protein. To examine further whether pterostilbene could induce other members of the Cdk inhibitor family, we investigated the effect of pterostilbene on the expression of p53, p21, p27, and p16 protein in AGS cells. The expression of p53, p21, p27, and p16 protein was significantly increased after exposure to 80 μM pterostilbene in a time-dependent manner (**Figure 7D**). Upon exposure to 80 μM pterostilbene, the levels of cyclin A1, D1, E, Cdk2, and Cdk4 were analyzed by immunoblotting over a 24 h period. The results revealed that cyclin D1 level did not

change with increasing time, while pterostilbene appeared to have a suppressing effect on the levels of cyclin A, E, Cdk2, Cdk4, and 6, which are associated with Rb phosphorylation.

DISCUSSION

Epidemiological studies have linked the consumption of fruits and vegetables to reduced risk of several types of human cancer. Laboratory animal studies have provided evidence that pterostilbene significantly suppressed azoxymethane-induced formation of ACF and multiple clusters of aberrant crypts and inhibited AOM-induced iNOS expression (*4*). Pterostilbene has been reported to exhibit many biological effects including anticancer activity, but their anticancer mechanism is still not clear. The results of the present study demonstrate that pterostilbene is a strong suppressor of human gastric carcinoma AGS cell proliferation. It is important to point out that growth inhibitory effects of pterostilbene were observed at concentrations that may be generated through dietary intake of berries. We also found that pterostilbene exerts activity against proliferation of AGS cells by causing apoptosis and arresting cells in the G_0/G_1 phase of the cell cycle.

Accumulating evidence clearly indicates that apoptosis is a critical molecular target for dietary bioactive agents for chemoprevention of cancer. Data generated from this research have clarified the molecular mechanism by which pterostilbene triggered human gastric carcinoma AGS cells to undergo apoptosis. As shown in **Figure 3**, pterostilbene is a strong inhibitor of cell viability and causes the potent and rapid induction of apoptosis, concurrent with DNA laddering, sub-G1 peak appearance, chromatin condensation, and apoptotic appearance in AGS cells. This induction of apoptosis occurs within hours, consistent with the view that pterostilbene induces apoptosis by activating preexisting apoptosis machinery. Herein, we demonstrated that pterostilbene could disruption the functions of mitochondria at the early stages of apoptosis and subsequently coordinate caspase-9 activation, but not caspase-1, through the release of cytochrome *c*. Indeed, treatment with pterostilbene caused an induction of caspase-2, -3, -6, and -8 (but not caspase-1) associated with the degradation of DFF-45 and PARP, which preceded the onset of apoptosis. Pretreatment with the pan-caspase inhibitor Z-VAD-FMK inhibited pterostilbene-induced apoptosis, suggesting that apoptosis induced by pterostilbene involves a caspase-3-mediated mechanism. The receptor-mediated signaling transduction pathway of apoptosis is another major pathway in activating caspase cascades. In our study, we observed the enhancement expression of Fas and FasL in pterostilbene-treated AGS cells (**Figure 5**).

It is well established that uncontrolled cellular growth as a consequence of defects in apoptosis and cell cycle machinery is responsible for the development of most of the cancers including gastric cancer. Cancer progression has been suggested to involve the loss of cell cycle checkpoint controls that regulate the passage through cell cycle. Checkpoints are control mechanisms that ensure the proper timing of cell cycle events and monitor the integrity of the DNA (*29*). The ER stress-induced cell death modulator is a CCAAT/enhancer-binding protein (CEBP) homology protein (CHOP)/growth GADD153, known as CHOP, which is a member of the CEBP family of transcription factors (*30*). There are three distinct GADD genes: GADD34, GADD45, and GADD153. Expressed at low levels in proliferating cells, it is strongly induced in response to stresses that result in growth arrest or cellular death, including oxidant injury (*31*), DNA damaging agents such as peroxynitrite (*32*), UV radiation (*33*), anticancer chemotherapy (*34*), and ER stress (*35, 36*). The cycle is regulated by inhibitory proteins, such as GADD, which are responsible for the maintenance of cell cycle checkpoints, preventing inappropriate mitosis. As an extracellular stress signal, pterostilbene induces ROS production and expression of GADD in AGS cells, leading to cell cycle arrest in G_0/G_1. These findings suggest that GADD expression triggered by pterostilbene-induced DNA damage and p53 expression (**Figure 7**). Thus, the increase in GADD45 and GADD153 provides a clue about the mechanism of the effects of pterostilbene.

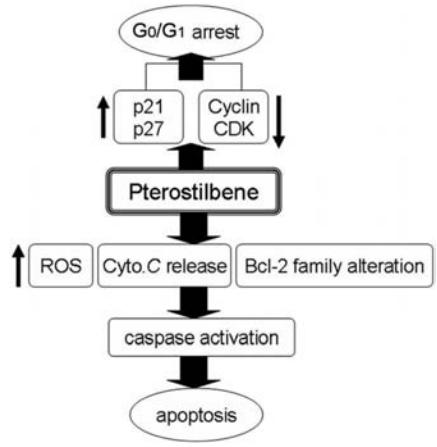

Figure 8. Proposed mechanisms of pterostilbene-induced apoptosis and G_0/G_1 arrest in AGS cells. See the text for details.

Base on the outcome of this study and the available literature, the mechanisms by which pterostilbene causes apoptosis and cell cycle arrest in AGS cells are summarized in **Figure 8**. We suggest that pterostilbene induces up-regulation of tumor suppressor, p53, cyclin kinase inhibitors $p21^{Cip1}$, $p27^{Kip1}$, and p16, in turn inhibiting cell cycle regulatory molecules resulting in G_1 arrest and apoptosis. Down-regulation of Cdk4/Cdk6 inhibits pRb, which inhibits protein expression of E2F family proteins, leading to gene transcription and apoptosis. Because Bax and Bcl-2 play a critical role in induction of apoptosis, alteration of the Bax/Bcl-2 ratio activates caspase signaling, resulting in apoptotic cell death. Hence, we conclude that pterostilbene would be an attractive agent for human gastric cancer research and possibly treatment.

ABBREVIATIONS USED

DFF, DNA fragmentation factor; PARP, poly(ADP-ribose) polymerase; Apaf-1, apoptotic protease activating factor 1; ICAD, inhibitor of caspase-3-activated DNase; DCHF-DA, dichlorodihydrofluorescein diacetate; ROS, reactive oxygen species; MTT, 3-(4,5-dimethylthiazol-2-yl)-2,5-diphenyltetrazolium bromide.

LITERATURE CITED

(1) Ferrer, P.; Asensi, M.; Segarra, R.; Ortega, A.; Benlloch, M.; Obrador, E.; Varea, M. T.; Asensio, G.; Jorda, L.; Estrela, J. M. Association between pterostilbene and quercetin inhibits metastatic activity of B16 melanoma. *Neoplasia* **2005**, *7* (1), 37–47.

(2) Rimando, A. M.; Cuendet, M.; Desmarchelier, C.; Mehta, R. G.; Pezzuto, J. M.; Duke, S. O. Cancer chemopreventive and antioxidant activities of pterostilbene, a naturally occurring analogue of resveratrol. *J. Agric. Food Chem.* **2002**, *50* (12), 3453–3457.

(3) Tolomeo, M.; Grimaudo, S.; Di, C. A.; Roberti, M.; Pizzirani, D.; Meli, M.; Dusonchet, L.; Gebbia, N.; Abbadessa, V.; Crosta, L.; Barucchello, R.; Grisolia, G.; Invidiata, F.; Simoni, D. Pterostilbene and 3′-hydroxypterostilbene are effective apoptosis-inducing agents in MDR and BCR-ABL-expressing leukemia cells. *Int. J. Biochem. Cell Biol.* **2005**, *37* (8), 1709–1726.

(4) Suh, N.; Paul, S.; Hao, X.; Simi, B.; Xiao, H.; Rimando, A. M.; Reddy, B. S. Pterostilbene, an active constituent of blueberries, suppresses aberrant crypt foci formation in the azoxymethane-induced colon carcinogenesis model in rats. *Clin. Cancer Res.* **2007**, *13* (1), 350–355.

(5) Rimando, A. M.; Kalt, W.; Magee, J. B.; Dewey, J.; Ballington, J. R. Resveratrol, pterostilbene, and piceatannol in vaccinium berries. *J. Agric. Food Chem.* **2004**, *52* (15), 4713–4719.

(6) Correa, P. Helicobacter pylori and gastric cancer: state of the art. *Cancer Epidemiol. Biomarkers Prev.* **1996**, *5* (6), 477–481.

(7) Howson, C. P.; Hiyama, T.; Wynder, E. L. The decline in gastric cancer: epidemiology of an unplanned triumph. *Epidemiol. Rev.* **1986**, *8*, 1–27.

(8) Review (226 refs): Kelloff, G. J.; Boone, C. W.; Crowell, J. A.; Steele, V. E.; Lubet, R.; Sigman, C. C. Chemopreventive drug development: perspectives and progress. *Cancer Epidemiol., Biomarkers Prev.* **1994**, *3* (1), 85–98.

(9) Kang, S. K.; Burnett, C. A.; Freund, E.; Walker, J.; Lalich, N.; Sestito, J. Gastrointestinal cancer mortality of workers in occupations with high asbestos exposures. *Am. J. Ind. Med.* **1997**, *31* (6), 713–718.

(10) Hirota, S. Gastrointestinal stromal tumors: their origin and cause. *Int. J. Clin. Oncol.* **2001**, *6* (1), 1–5.

(11) Strickland, L.; Letson, G. D.; Muro-Cacho, C. A. Gastrointestinal stromal tumors. *Cancer Control* **2001**, *8* (3), 252–261.

(12) Green, D. R.; Evan, G. I. A matter of life and death. *Cancer Cell* **2002**, *1* (1), 19–30.

(13) Ricci, J. E.; Munoz-Pinedo, C.; Fitzgerald, P.; Bailly-Maitre, B.; Perkins, G. A.; Yadava, N.; Scheffler, I. E.; Ellisman, M. H.; Green, D. R. Disruption of mitochondrial function during apoptosis is mediated by caspase cleavage of the p75 subunit of complex I of the electron transport chain. *Cell* **2004**, *117* (6), 773–786.

(14) Rao, R. V.; Ellerby, H. M.; Bredesen, D. E. Coupling endoplasmic reticulum stress to the cell death program. *Cell Death Differ.* **2004**, *11* (4), 372–380.

(15) Nakagawa, T.; Zhu, H.; Morishima, N.; Li, E.; Xu, J.; Yankner, B. A.; Yuan, J. Caspase-12 mediates endoplasmic-reticulum-specific apoptosis and cytotoxicity by amyloid-beta. *Nature (London)* **2000**, *403* (6765), 98–103.

(16) Kaufman, R. J. Stress signaling from the lumen of the endoplasmic reticulum: coordination of gene transcriptional and translational controls. *Genes Dev.* **1999**, *13* (10), 1211–1233.

(17) Morgan, D. O. Principles of CDK regulation. *Nature (London)* **1995**, *374* (6518), 131–134.

(18) Pettit, G. R.; Grealish, M. P.; Jung, M. K.; Hamel, E.; Pettit, R. K.; Chapuis, J. C.; Schmidt, J. M. Antineoplastic agents. 465. Structural modification of resveratrol: sodium resverastatin phosphate. *J. Med. Chem.* **2002**, *45* (12), 2534–2542.

(19) Pan, M. H.; Huang, M. C.; Wang, Y. J.; Lin, J. K.; Lin, C. H. Induction of apoptosis by hydroxydibenzoylmethane through coordinative modulation of cyclin D3, Bcl-X(L), and Bax, release of cytochrome c, and sequential activation of caspases in human colorectal carcinoma cells. *J. Agric. Food Chem.* **2003**, *51* (14), 3977–3984.

(20) Pan, M. H.; Chang, W. L.; Lin-Shiau, S. Y.; Ho, C. T.; Lin, J. K. Induction of apoptosis by garcinol and curcumin through cytochrome c release and activation of caspases in human leukemia HL-60 cells. *J. Agric. Food Chem.* **2001**, *49* (3), 1464–1474.

(21) Pan, M. H.; Lin, J. H.; Lin-Shiau, S. Y.; Lin, J. K. Induction of apoptosis by penta-O-galloyl-beta-D-glucose through activation of caspase-3 in human leukemia HL-60 cells. *Eur. J. Pharmacol.* **1999**, *381* (2–3), 171–183.

(22) Green, D. R.; Reed, J. C. Mitochondria and apoptosis. *Science* **1998**, *281* (5381), 1309–1312.

(23) Martindale, J. L.; Holbrook, N. J. Cellular response to oxidative stress: signaling for suicide and survival. *J. Cell Physiol.* **2002**, *192* (1), 1–15.

(24) Li, P.; Nijhawan, D.; Budihardjo, I.; Srinivasula, S. M.; Ahmad, M.; Alnemri, E. S.; Wang, X. Cytochrome c and dATP-dependent formation of Apaf-1/caspase-9 complex initiates an apoptotic protease cascade. *Cell* **1997**, *91* (4), 479–489.

(25) Enari, M.; Talanian, R. V.; Wong, W. W.; Nagata, S. Sequential activation of ICE-like and CPP32-like proteases during Fas-mediated apoptosis. *Nature (London)* **1996**, *380* (6576), 723–726.

(26) Liu, X.; Zou, H.; Slaughter, C.; Wang, X. DFF, a heterodimeric protein that functions downstream of caspase-3 to trigger DNA fragmentation during apoptosis. *Cell* **1997**, *89* (2), 175–184.

(27) Sakahira, H.; Enari, M.; Nagata, S. Cleavage of CAD inhibitor in CAD activation and DNA degradation during apoptosis. *Nature (London)* **1998**, *391* (6662), 96–99.

(28) Nagata, S. Apoptosis by death factor. *Cell* **1997**, *88* (3), 355–365.

(29) Molinari, M. Cell cycle checkpoints and their inactivation in human cancer. *Cell Prolif.* **2000**, *33* (5), 261–274.

(30) Wang, X. Z.; Lawson, B.; Brewer, J. W.; Zinszner, H.; Sanjay, A.; Mi, L. J.; Boorstein, R.; Kreibich, G.; Hendershot, L. M.; Ron, D. Signals from the stressed endoplasmic reticulum induce C/EBP-homologous protein (CHOP/GADD153). *Mol. Cell Biol.* **1996**, *16* (8), 4273–4280.

(31) Ikeyama, S.; Wang, X. T.; Li, J.; Podlutsky, A.; Martindale, J. L.; Kokkonen, G.; van, H. R.; Gorospe, M.; Holbrook, N. J. Expression of the pro-apoptotic gene gadd153/chop is elevated in liver with aging and sensitizes cells to oxidant injury. *J. Biol. Chem.* **2003**, *278* (19), 16726–16731.

(32) Oh-Hashi, K.; Maruyama, W.; Isobe, K. Peroxynitrite induces GADD34, 45, and 153 VIA p38 MAPK in human neuroblastoma SH-SY5Y cells. *Free Radical Biol. Med.* **2001**, *30* (2), 213–221.

(33) Tong, T.; Fan, W.; Zhao, H.; Jin, S.; Fan, F.; Blanck, P.; Alomo, I.; Rajasekaran, B.; Liu, Y.; Holbrook, N. J.; Zhan, Q. Involvement of the MAP kinase pathways in induction of GADD45 following UV radiation. *Exp. Cell Res.* **2001**, *269* (1), 64–72.

(34) Kim, D. G.; You, K. R.; Liu, M. J.; Choi, Y. K.; Won, Y. S. GADD153-mediated anticancer effects of N-(4-hydroxyphenyl) retinamide on human hepatoma cells. *J. Biol. Chem.* **2002**, *277* (41), 38930–38938.

(35) McCullough, K. D.; Martindale, J. L.; Klotz, L. O.; Aw, T. Y.; Holbrook, N. J. Gadd153 sensitizes cells to endoplasmic reticulum stress by down-regulating Bcl2 and perturbing the cellular redox state. *Mol. Cell Biol.* **2001**, *21* (4), 1249–1259.

(36) Wang, X. Z.; Lawson, B.; Brewer, J. W.; Zinszner, H.; Sanjay, A.; Mi, L. J.; Boorstein, R.; Kreibich, G.; Hendershot, L. M.; Ron, D. Signals from the stressed endoplasmic reticulum induce C/EBP-homologous protein (CHOP/GADD153). *Mol. Cell Biol.* **1996**, *16* (8), 4273–4280.

Received for review May 24, 2007. Revised manuscript received July 16, 2007. Accepted July 17, 2007. This study was supported by the National Science Council NSC 95-2321-B-022-001 and NSC 95-2313-B-022-003-MY3.

JF071520H